British Journal of Pharmacology

DOI:10.1111/j.1476-5381.2011.01449.x
www.brjpharmacol.org

RESEARCH PAPER

Celastrol inhibits proliferation and induces chemosensitization through down-regulation of NF-κB and STAT3 regulated gene products in multiple myeloma cells

Radhamani Kannaiyan[1]*, Hui Sin Hay[2]*, Peramaiyan Rajendran[1], Feng Li[1], Muthu K Shanmugam[1], Shireen Vali[3,4], Taher Abbasi[3,4], Shweta Kapoor[4], Ashish Sharma[4], Alan Prem Kumar[1,2], Wee-Joo Chng[2,5] and Gautam Sethi[1,2]

[1]*Department of Pharmacology, Yong Loo Lin School of Medicine, National University of Singapore, Singapore,* [2]*Cancer Science Institute of Singapore, National University of Singapore, Singapore,* [3]*Cellworks Group Inc., Saratoga, CA, USA,* [4]*Cellworks Research India Pvt. Ltd, Bangalore, India, and* [5]*Department of Haematology-Oncology, National University Cancer Institute, Singapore, National University Health System, Singapore*

Correspondence
Dr Gautam Sethi, Department of Pharmacology, Yong Loo Lin School of Medicine, Cancer Science Institute of Singapore, National University of Singapore, 10 Medical Drive, Singapore 11759. E-mail: phcgs@nus.edu.sg; Dr Wee-Joo Chng, Department of Haematology-Oncology, National University Cancer Institute, Singapore, National University Health System, Singapore. E-mail: mdccwj@nus.edu.sg; Dr Alan Prem Kumar, Department of Pharmacology, Yong Loo Lin School of Medicine, Cancer Science Institute of Singapore, National University of Singapore, 10 Medical Drive, Singapore 11759. E-mail: csiapk@nus.edu.sg

*Both R. K. and H. S. H. contributed equally to this work.

Keywords
celastrol; multiple myeloma; NF-κB; STAT3

Received
8 September 2010
Revised
31 March 2011
Accepted
4 April 2011

BACKGROUND AND PURPOSE

Activation of pro-inflammatory transcription factors NF-κB and signal transducer and activator of transcription 3 (STAT3) is one of the major contributors to both pathogenesis and chemoresistance in multiple myeloma (MM), which results in high mortality rate. Thus, in the present study, we investigated whether celastrol could suppress the proliferation and induce chemosensitization of MM cells by interfering with NF-κB and STAT3 activation pathways.

EXPERIMENTAL APPROACH

The effects of celastrol were investigated using both a virtual predictive tumour cell system and different MM cell lines resistant to doxorubicin, melphalan and bortezomib.

KEY RESULTS

Celastrol inhibited the proliferation of MM cell lines regardless of whether they were sensitive or resistant to bortezomib and other conventional chemotherapeutic drugs. It also synergistically enhanced the apoptotic effects of thalidomide and bortezomib. This correlated with the down-regulation of various proliferative and anti-apoptotic gene products including cyclin D1, Bcl-2, Bcl-xL, survivin, XIAP and Mcl-1. These effects of celastrol were mediated through suppression of constitutively active NF-κB induced by inhibition of IκBα kinase activation; and the phosphorylation of IκBα and of p65. Celastrol also inhibited both the constitutive and IL6-induced activation of STAT3, which induced apoptosis as indicated by an increase in the accumulation of cells in the sub-G1 phase, an increase in the expression of pro-apoptotic proteins and activation of caspase-3.

CONCLUSIONS AND IMPLICATIONS

Thus, based on our experimental findings, we conclude that celastrol may have great potential as a treatment for MM and other haematological malignancies.

Abbreviations

JAK, janus-like kinase; MM, multiple myeloma; MTT, 3-(4,5-dimethylthiazol-2-yl)-2,5-diphenyl-2H-tetrazolium bromide; STAT3, signal transducer and activator of transcription 3

Introduction

Multiple myeloma (MM) is a clonal plasma cell malignancy clinically characterized by osteolytic lesions, immunodeficiency and renal disease (Kyle and Rajkumar, 2004, 2008; Raab *et al.*, 2009). There are an estimated 750 000 people diagnosed with MM worldwide, with a median overall survival of 3–5 years (Raab *et al.*, 2009; Jagannath *et al.*, 2010). Although existing treatment modalities, including thalidomide, lenalidomide, bortezomib and autologous transplantation result in an improvement in overall survival of patients (Jagannath, 2005; Kumar and Rajkumar, 2006; Shah and Orlowski, 2009), the majority of patients eventually experience a relapse, their disease becomes chemoresistant, and they ultimately die of the disease (Raab *et al.*, 2009; Sung *et al.*, 2009).

The precise molecular mechanism(s) underlying chemoresistance in MM is not clear, but the activation of transcription factors (NF-κB and STAT3), and dysregulation of apoptosis have been implicated as the major players involved in chemoresistance (Catlett-Falcone *et al.*, 1999; Ni *et al.*, 2001; Bhardwaj *et al.*, 2007; Conticello *et al.*, 2011). Chemoresistance may also involve IL-6, the expression of which is induced by NF-κB (Kawano *et al.*, 1988) and leads to constitutive activation of STAT3, which in turn results in expression of high levels of Bcl-xL (Catlett-Falcone *et al.*, 1999). Thus, the use of anticancer agents derived from natural sources may be able to overcome resistance without some of the adverse side effects of conventional chemotherapy in MM patients.

One such agent is celastrol, a triterpene derived from the Chinese medicinal plant *Tripterygium wilfordii*, which has attracted great attention lately for its potent anticancer effects (Sethi *et al.*, 2007a; Kannaiyan *et al.*, 2010). Celastrol has been found to inhibit the proliferation of a variety of tumour cells and to suppress the growth of prostate, gliomas and chronic myeloid leukaemia xenografts in nude mice models (Huang *et al.*, 2008; Lu *et al.*, 2010; Pang *et al.*, 2010). The ability of celastrol to modulate the expression of pro-inflammatory cytokines, adhesion molecules, potassium channels, NF-κB, transforming growth factor activated kinase 1 (TAK1), CXCR4, VEGFR, proteasome and heat shock response has been previously reported (Sethi *et al.*, 2007a; Huang *et al.*, 2008; Morita *et al.*, 2008; Kannaiyan *et al.*, 2010; Li-Weber, 2010; Salminen *et al.*, 2010; Yadav *et al.*, 2010).

Whether celastrol can modulate proliferation of human MM cells or overcome the resistance of such cells to chemotherapy is not known. Alongside testing the effects of celastrol in MM cell lines, we also tested the hypothesis that inhibition of NF-κB and STAT3 is involved in celastrol's mechanism of action in a virtual predictive tumour cell system. The virtual epithelial tumour cell platform on which predictive studies were conducted to determine the various targets being modulated by celastrol is a comprehensive integrated representation of the pathways in key cancer phenotypes of proliferation, apoptosis, angiogenesis, metastasis and conditions of tumour microenvironment including tumour-associated inflammation (Cirstea *et al.*, 2010). This is a dynamic network of pathways with inter- and intracellular crosstalk and associated autocrine and paracrine loops whereby any internal marker can be perturbed through % knock-down and over-expression and an effect seen on the whole network. This virtual tumour cell has been used to get an insight into how a particular drug individually or in combination affects various cancer phenotypes across different tumour profiles (Roy *et al.*, 2010; Vali *et al.*, 2010). Thus, using a novel approach, the combination of predictive virtual hypothesis testing along with experimental validations, we found that celastrol can indeed inhibit the proliferation and overcome the chemoresistance of MM cells, and these effects occurred through the suppression of NF-κB and STAT3, which in turn leads to the down-regulation of anti-apoptotic gene products.

Methods

Reagents

Celastrol with purity greater than 98% was purchased from Alexis Biochemicals (San Diego, CA, USA). RPMI 1640, 0.4% trypan blue vital stain, and antibiotic–antimycotic mixture were obtained from Invitrogen (Carlsbad, CA, USA). Propidium iodide (PI), thalidomide and β-actin antibody was obtained from Sigma-Aldrich Chemical Co. (St. Louis, MO, USA). Fetal bovine serum (FBS) was purchased from BioWest (Miami, FL, USA).

Antibodies against phospho-STAT3 (Tyr 705), phospho-Akt (Ser 473), IκBα, Bax, Bak, Bcl-2, Bcl-xL, survivin, XIAP, Mcl-1, PARP, Akt, STAT-3, GAPDH, Lamin B and Annexin V-FITC assay kit were obtained from Santa Cruz Biotechnology (Santa Cruz, CA, USA). Antibodies to phospho-specific Src (Tyr 416), Src, phospho-specific JAK2 (Tyr 1007/1008) and JAK2, phospho-specific p65 (Ser 536) and p65, phospho-specific IκBα (Ser 32/36), phospho-specific IKKα/β (Ser 180/Ser 181), IKKα were purchased from Cell Signaling Technology (Beverly, MA, USA). Nuclear extraction and DNA binding kits were obtained from Active Motif (Carlsbad, CA, USA). Bortezomib (Velcade, PS341) was purchased from LC Laboratories (Woburn, MA, USA).

Cell lines and culture conditions

The human MM cell lines U266 and RPMI 8226, RPMI-8226-Dox-6 (a doxorubicin-resistant clone) and RPMI-8226-LR-5 (a melphalan-resistant clone) were kindly provided by Dr Leif Bergsagel from Mayo Clinic, Arizona, USA. RPMI-8226-

bortezomib resistant clones were kindly provided by Dr Jacqueline Cloos from Vrije Universiteit Medical Center, Amsterdam, the Netherlands. All the human MM cells were cultured in RPMI 1640 medium containing 1 × antibiotic–antimycotic with 10% FBS. Mouse embryonic fibroblasts (MEFs) were a kind gift from Professor Bharat B. Aggarwal from M.D. Anderson Cancer Center, Houston, Texas and were cultured in DMEM medium containing 1 × antibiotic–antimycotic with 10% FBS.

In silico *analysis*

The Cellworks tumour cell platform provides a dynamic and transparent view of human cellular physiology at the proteomics abstraction level. The virtual tumour cell platform consists of a dynamic and kinetic representation of the signalling pathways underlying tumour physiology at the biomolecular level. The platform has been correlated against an extensive set of predefined *in vitro* and *in vivo* studies (Cirstea *et al.*, 2010).

Platform description

The virtual tumour cell platform consists of a dynamic and kinetic representation of the signalling pathways underlying tumour physiology at the bio-molecular level. All the key relevant protein players and associated gene and mRNA species with regard to tumour-related signalling are comprehensively included in the system with their relationship quantitatively represented. Pathways and signalling for different cancer phenotypes comprise 75 major signalling networks with more than 3900 intracellular molecules. The platform includes important signalling pathways comprising growth factors like EGFR, PDGFRA, FGFR, c-MET, VEGFR and IGF-1R, cell cycle regulators, mTOR signalling, p53 signalling cascade, cytokine pathways like IL-1, IL-4, IL-6, IL-12, TNF, lipid mediators and tumour metabolism. The modelling of the time-dependent changes in the fluxes of the constituent pathways has been done utilizing modified ordinary differential equations and mass action kinetics. The platform has been correlated against an extensive set of predefined *in vitro* and *in vivo* studies.

Study details

The base line used for the study was a BRAF over-expressed, RB1 and P53 mutant, aligned to U266 cell line (Yu *et al.*, 2010; Zhang *et al.*, 2010). The following studies were conducted in disease state and the biomarker trends evaluated as percentage change from disease values.

- HSP90 activity was inhibited by 80%
- NF-κB activation was inhibited by 80%
- HO-1 expression was induced to increase twofold
- A combination of the HSP90 and NF-κB inhibition, NF-κB inhibition and HO-1 induction, HSP90 inhibition with HO-1 induction and all the three in combination was also tested along with the above three individual experiments

The results for the above studies individually or in combination were analysed across known biomarker trends for celastrol and the trends were compared with known literature.

MTT assay

The antiproliferative effects of celastrol on drug-sensitive and drug-resistant MM cells were determined by the MTT dye uptake method as described previously (Li *et al.*, 2010).

Western blotting

For detection of various proteins, celastrol-treated whole-cell extracts were lysed in lysis buffer [20 mM Tris (pH 7.4), 250 mM NaCl, 2 mM EDTA (pH 8.0), 0.1% Triton X-100, 0.01 mg·mL^{-1} aprotinin, 0.005 mg·mL^{-1} leupeptin, 0.4 mM PMSF, and 4 mM $NaVO_4$]. Lysates were then spun at 17 000× *g* for 10 min and resolved on a SDS gel. After electrophoresis, the proteins were electrotransferred to a nitrocellulose membrane, blocked with 5% non-fat milk, and probed with various primary antibodies (1:1000) overnight at 4°C. The blot was washed, exposed to horseradish peroxidase-conjugated secondary antibodies for 1 h, and finally examined by chemiluminescence (ECL; GE Healthcare, Little Chalfont, Buckinghamshire, UK). The densitometric analysis of the scanned blots was done using Image J software and the results are expressed as fold change relative to the control.

NF-κB DNA binding assay

To determine NF-κB activation, we performed a DNA binding assay as previously described (Renard *et al.*, 2001). Briefly, the binding of NF-κB to DNA was measured in nuclear extracts with a fast, user-friendly, ELISA-based TransAM NF-κB p65 assay kit (Active Motif Inc.). This assay uses multiwell plates coated with an unlabeled oligonucleotide containing the consensus binding site for NF-κB (5′-GGGACTTTCC-3′). Nuclear proteins (20 µg) were added to each well and incubated for 1 h to allow NF-κB DNA binding. Subsequently, by using an antibody that is directed against NF-κB p65 subunit, the NF-κB complex bound to the oligonucleotide is detected. A horseradish peroxidase-conjugated secondary antibody provided the basis for the colorimetric quantification.

Immunocytochemistry for NF-κB p65 and STAT3 localization

MM cell lines were examined for NF-κB and for STAT3 by an immunocytochemistry method essentially as described previously (Bharti *et al.*, 2003).

RNA extraction and real-time PCR analysis

Total RNA was extracted using the Trizol reagent (Invitrogen, Carlsbad, CA, USA), according to the manufacturer's instructions. Reverse transcription was then carried out as described previously (Kumar *et al.*, 2009). Briefly, for a 50 µL reaction, 10 µL of RT product was mixed with 1 × TaqMan® Universal PCR Master mix, 2.5 µL of 20 × TaqMan probes for Bcl-2, Bcl-xl, survivin and Mcl-1, respectively, 2.5 µL of 20 × 18S RNA TaqMan probe as the endogenous control for each targeting gene, and topped up to 50 µL with sterile water. A negative control for RT, in which sterile water replaced the RNA template, was included. Another control, where RT mix was replaced with sterile water, was included to check for DNA contamination. Real-time PCR was done using 7500 Fast Real-Time PCR System (ABI PRISM 7500, Applied Biosystems, Foster City, CA, USA) with a protocol that consists of 50°C for

2 min, 95°C for 10 min, followed by 40 cycles of denaturing at 95°C for 15 s and extension at 60°C for 1 min. Results were analysed using Sequence Detection Software version 1.3 provided by Applied Biosystems. Relative gene expression was obtained after normalization with endogenous 18S RNA and determination of the difference in threshold cycle (Ct) between treated and untreated cells using 2-ΔΔCt method. Primers and probes for human Bcl-2, Bcl-xL, survivin and Mcl-1, were purchased as kits from Applied Biosystems (Assays-on-Demand).

Live/Dead assay

Apoptosis of cells was also determined by the Live/Dead assay (Molecular Probes, Eugene, OR, USA) as described previously (Tan *et al.*, 2010).

Annexin V assay

One of the early indicators of apoptosis is the rapid translocation and accumulation of the membrane phospholipid phosphatidylserine from the cytoplasmic interface to the extracellular surface. This loss of membrane asymmetry can be detected by utilizing the binding properties of annexin V. This assay was performed as described previously (Sethi *et al.*, 2007a).

Flow cytometric analysis

To determine the effect of celastrol on the cell cycle distribution, MM and MEF cells were first exposed to celastrol for the indicated time intervals. Thereafter cells were washed, fixed with 70% ethanol, and incubated for 30 min at 37°C with 0.1% RNase A in PBS. Cells were then washed again, resuspended, and stained in PBS containing 50 $\mu g \cdot mL^{-1}$ PI for 30 min at room temperature. Cell distribution across the cell cycle was analysed with CyAn ADP flow cytometer (Dako Cytomation).

Statistical analysis

Statistical analysis was performed by Student's unpaired *t*-test and one way analysis of variance (ANOVA) internal comparisons were done by Bonferroni Method. A probability (*P*) value less than 0.05 was considered statistically significant.

Results

The goal of this study was to determine whether celastrol can sensitize drug-resistant MM cells through the regulation of NF-κB and STAT3 activation. The anti-MM effects of celastrol were tested using virtual tumour cell platform to determine if indeed the effects are mediated either by inhibition of NF-κB or STAT3 or both, and predictive trends were compared with the experimental data. The chemical structure of celastrol has been published by our group previously (Sethi *et al.*, 2007b; Kannaiyan *et al.*, 2010).

Predictive analysis of HSP90 activity knock-down along with HO-1 induction

The HSP90 activity was inhibited by 55% and 92% along with the induced increased expression of HO-1 by twofold, in a BRAF over-expressed, RB1 and P53 mutant virtual tumour cell aligned to U266 cell. Figure 1A illustrates a high-level view of the virtual tumour cell platform. Figure 1B upper panel clearly shows that knocking down HSP90 activity by 55% and 92% along with HO-1 induction causes a reduction in NF-κB activity. Active phosphorylated STAT3, JAK2 and Src were all show reduced (Figure 1B, lower panel), and also all the key survival markers including Bcl-2, Bcl-xL, XIAP and survivin (BIRC5) were decreased with Hsp90 inhibition (Figure 1C, upper panel). Also, increased predictive trends were observed for the apoptotic markers caspase-3 and cleaved-PARP1 (Figure 1C, lower panel). Only the inhibition of HSP90 along with an induction of HO-1 caused a significant inhibition of NF-κB and STAT3 and the biomarker trends corroborated with the empirical results. These predictions support the hypothesis that modulation of various proliferative and apoptotic phenotypes by celastrol are mediated through inhibition of NF-κB and STAT3 activation.

Celastrol suppresses the proliferation of drug-resistant MM cell lines and synergistically enhances the apoptotic effects of thalidomide and bortezomib

Celastrol suppressed the proliferation of all MM cell types tested, including U266, RPMI 8226-Dox6 cells (resistant to doxorubicin), and RPMI 8226-LR5 cells (resistant to melphalan) and RPMI cell lines resistant to bortezomib in a dose- and time-dependent manner (Figure 2A).

Thalidomide (an inhibitor of TNF expression), and bortezomib (a proteasome inhibitor) have been approved by the Food and Drug Administration for the treatment of MM patients (Cavo and Baccarani, 2006; Glasmacher *et al.*, 2006). Whether celastrol can potentiate the effect of these drugs was examined. For this, U266 cells were treated with celastrol together with different concentrations of either thalidomide or bortezomib; and then examined for apoptosis using live and dead analysis, annexin V staining and cell cycle analysis. The results of live and dead, annexin V and cell cycle analysis clearly indicate that celastrol can substantially potentiate the apoptotic effects of both thalidomide and bortezomib (Figure 2B, C and D, left panel). Based on cell cycle analysis isobologram-illustrated results, we found that celastrol synergistically induced the accumulation of MM cells in sub-G1 phase when used in combination with thalidomide and bortezomib for 24 h (Figure 2D, right panel).

Celastrol causes accumulation of MM cells in the sub-G1 phase, increases expression of pro-apoptotic proteins and activates caspase-3

To further confirm that celastrol inhibits proliferation of MM cells through induction of apoptosis, we analysed cell cycle distribution after PI staining. We found that celastrol increased the accumulation of the cell population in the sub-G1 phase after the treatment with U266 for 12 h and 24 h (Figure 3A) and bortezomib-resistant RPMI-8226 cells for 24 h and 48 h (Figure 3B). However, celastrol did not induce a substantial accumulation of MEF cells in the sub-G1 phase after treatment for 12 h and 24 h, respectively, thereby indicating it does not have a toxic effect on normal cells (Figure 3C).

Increased expression of pro-apoptotic proteins Bax and Bak, was also seen in time-dependent manner after treatment

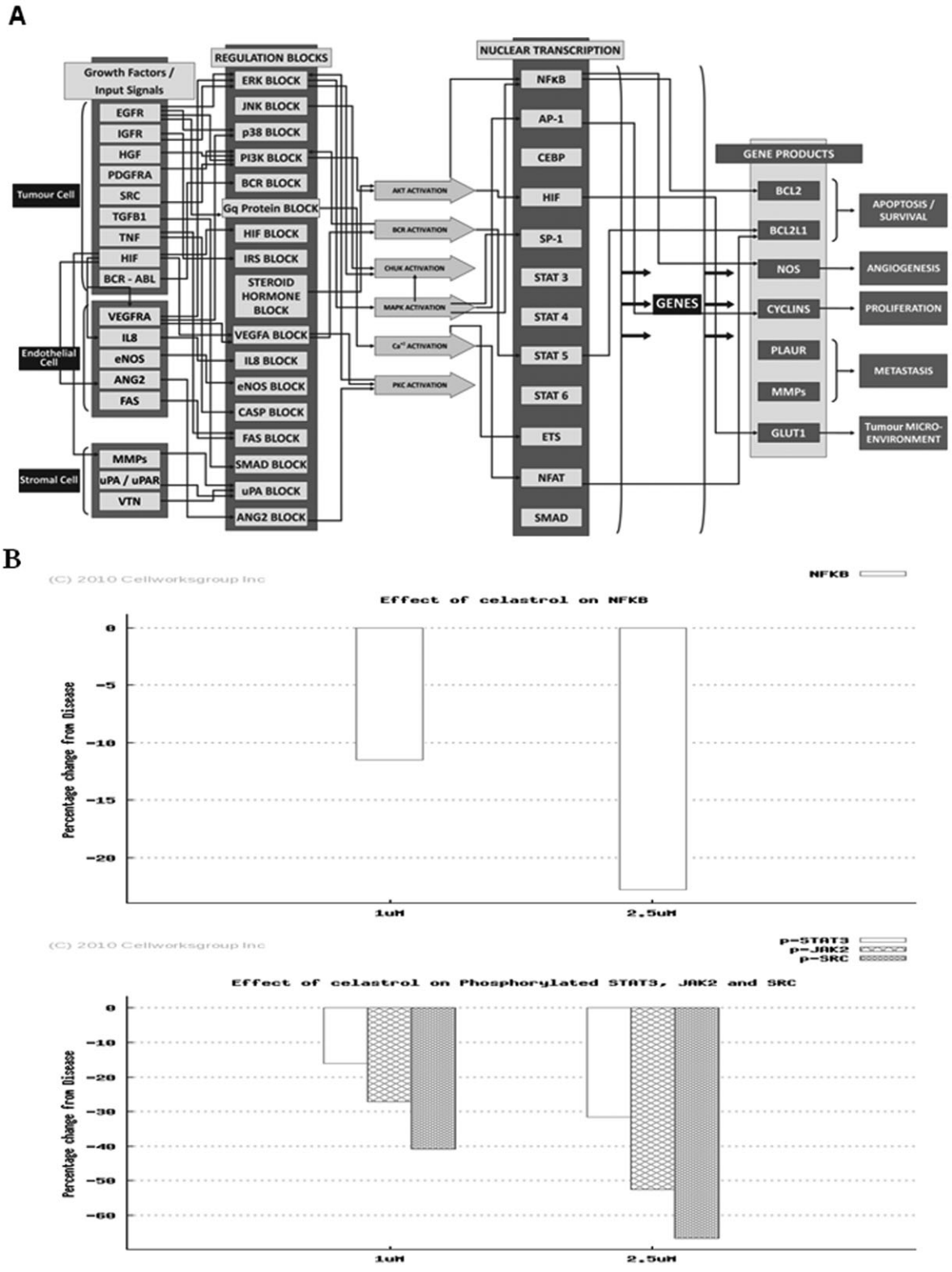

Figure 1

Predictive *in silico* virtual tumour platform generated results. (A) High-level view of the virtual tumour cell platform. (B, upper panel) The percentage reduction in NF-κB activity following HSP90 inhibition and HO-1 induction. (B, lower panel) The percentage reduction in phosphorylated STAT3, JAK2 and SRC kinase. (C, upper panel) The percentage reduction in survival markers-Bcl-2, Bcl-xL, XIAP and survivin. (C, lower panel) The percentage increase in caspase-3 and cleaved-PARP1 and the increasing trend of these markers supports the increase in apoptotic endpoint seen experimentally.

C

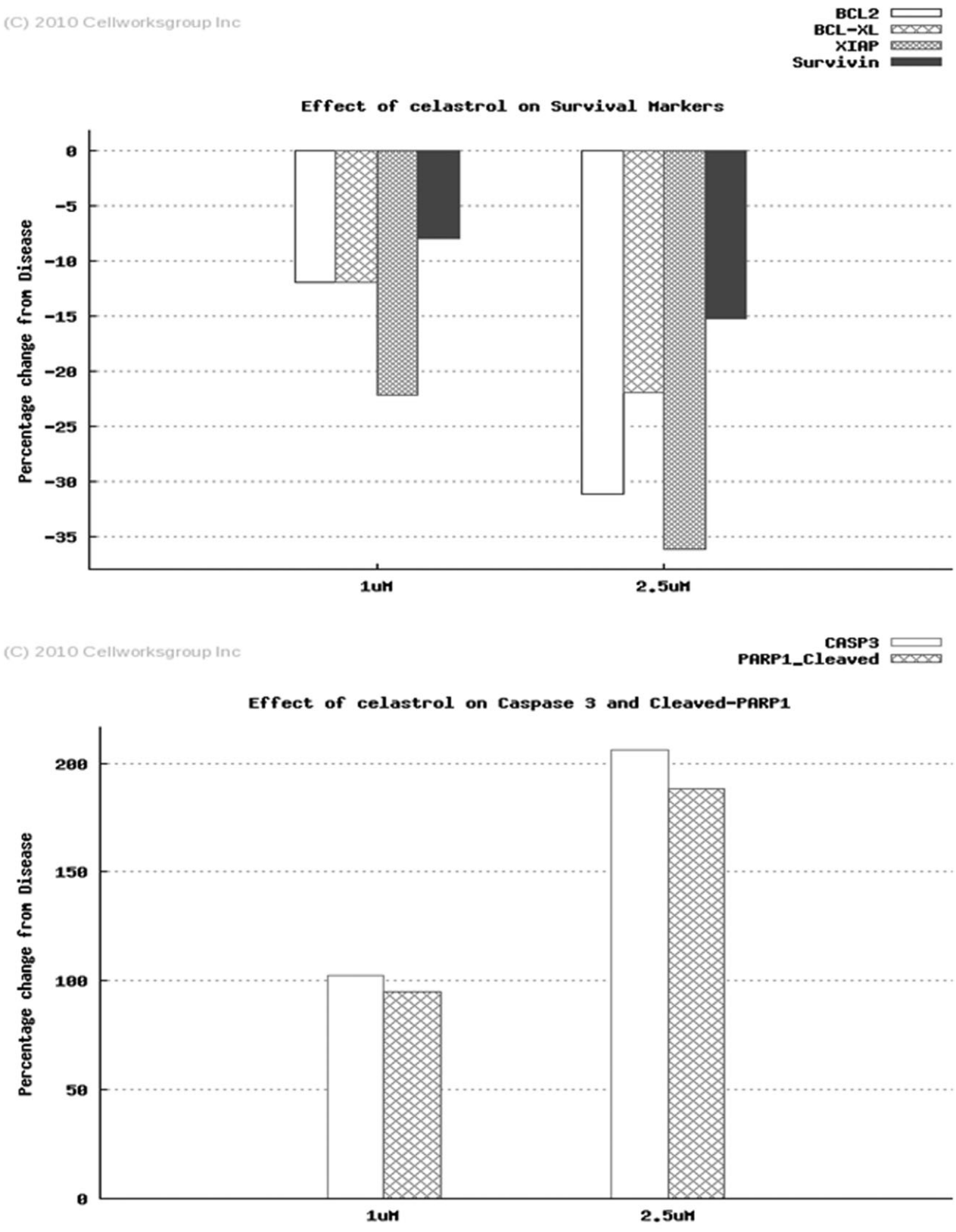

Figure 1
Continued.

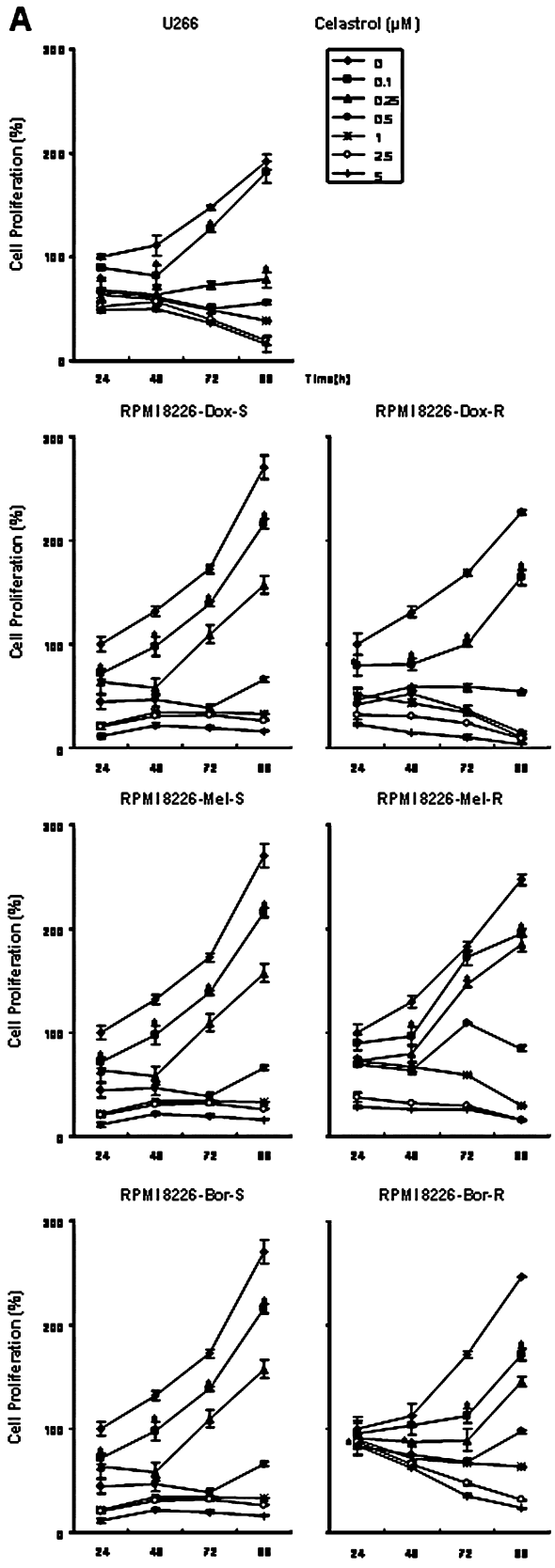

Figure 2

Celastrol suppresses the proliferation of drug-resistant MM cell lines and potentiates the effect of thalidomide and bortezomib. (A) U266 cells (5×10^3 100 μL^{-1}); doxorubicin-sensitive and doxorubicin-resistant RPMI 8266 cells (20×10^3 100 μL^{-1}); and melphalan-sensitive and melphalan-resistant bortezomib-sensitive and bortezomib-resistant RPMI 8226 cells were plated in triplicate, treated with 0, 0.1, 0.25, 0.5, 1, 2.5 and 5 μM celastrol, and then subjected to MTT assay on days 0, 1, 2, 3 and 4 to analyse proliferation of cells. Cell survival at all four days in the celastrol-treated group was significantly decreased as compared with the control group (*$P < 0.05$). (B) U266 cells (1×10^6 mL^{-1}) were treated with 0.5 μM celastrol, and 10 $\mu g \cdot mL^{-1}$ thalidomide or 10 nM bortezomib alone or in combination for 24 h at 37°C. Cells were stained with a Live/Dead assay reagent for 30 min and then analysed under a fluorescence microscope as described in Methods. (C) U266 cells (1×10^6 mL^{-1}) were treated with 0.5 μM celastrol, and 10 $\mu g \cdot mL^{-1}$ thalidomide (left panel) or 10 nM bortezomib (right panel) alone or in combination for 24 h at 37°C. Cells were incubated with anti-annexin V antibody conjugated with FITC and then analysed with a flow cytometer. * $P < 0.05$, ** $P < 0.005$. (D, left panel) U266 cells were treated with 0.5 μM celastrol, 10 $\mu g \cdot mL^{-1}$ and 20 $\mu g \cdot mL^{-1}$ thalidomide or 10 nM, and 20 nM bortezomib alone or in combination for 24 h at 37°C after which the cells were washed, fixed, stained with PI, and analysed for DNA content by flow cytometry. The representative histograms are shown only for thalidomide (10 $\mu g \cdot mL^{-1}$), bortezomib (10 nM) alone or in combination with celastrol (0.5 μM). The percentage of cells in the sub-G1 phase were used to calculate the combination index (CI). (D, right panel) Assessment of the type of combination relationship was done using the method developed by Chou–Talalay which used a multiple drug effect equation. The degree of synergy was assessed based on CI values, where a CI value of >1.0 implies antagonism, 1.0 implies additive and <1.0 implies synergistic effect.

with celastrol (Figure 3D). Celastrol also induced cleavage of procaspase-3 and PARP in U266 cells (Figure 3E), which suggests that celastrol induces apoptosis through the activation of caspases.

Celastrol suppresses Akt activation and inhibits the expression of anti-apoptotic proteins in MM cells

Activation of Akt also plays a major role in cell survival (Yamaguchi and Wang, 2001). Hence, we investigated whether celastrol modulates the activation of Akt in MM cells. Akt was found to be constitutively active in U266 cells and celastrol suppressed these constitutively phosphorylated Akt levels in a time-dependent manner (Figure 4A), thereby indicating that reduced Akt activation may contribute towards apoptosis of MM cells.

The effect of celastrol on the expression of genes implicated in tumour cell proliferation and survival was also investigated. We found that celastrol down-regulated the constitutive expression of cyclin D1 and anti-apoptotic gene products (Bcl-2, Bcl-xL, survivin, XIAP and Mcl-1) in a time-dependent manner in U266 cells (Figure 4B). We also found that mRNA expression of Bcl-2, Bcl-xL, survivin and Mcl-1 was modulated by celastrol with a maximum reduction observed after 6 h of treatment (Figure 4C). These results

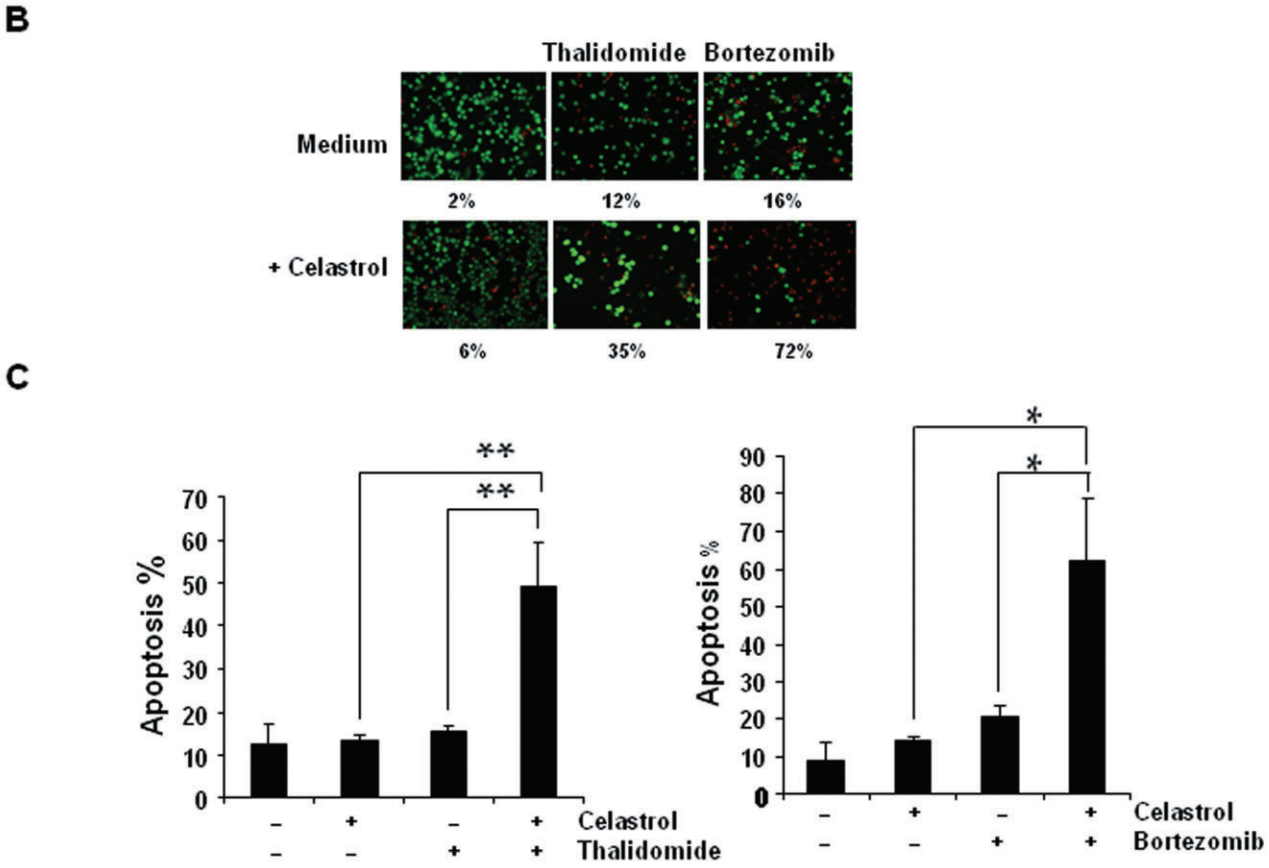

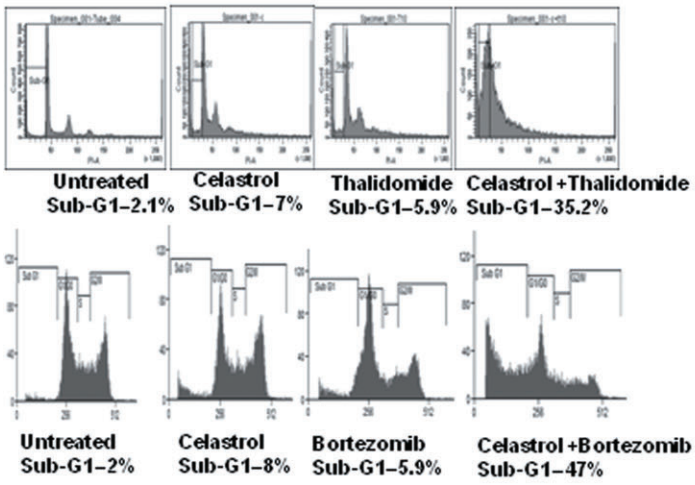

Cell line	Drugs	Dose	CI value	Relationship
U266	Celastrol	0.5 μM	n/a	n/a
	Thalidomide	10 μg·mL^{-1}	n/a	n/a
	Bortezomib	10 nM	n/a	n/a
	Celastrol+ Thalidomide	0.5 μM+ 10 μg·mL^{-1}	454E-6	Highly Synergistic
	Celastrol+ Thalidomide	0.5 μM+ 20 μg·mL^{-1}	0.068	Synergistic
	Celastrol+ Bortezomib	0.5 μM+ 10 nM	117E-5	Highly Synergistic
	Celastrol+ Bortezomib	0.5 μM+ 20 nM	0.0058	Synergistic

Figure 2
Continued.

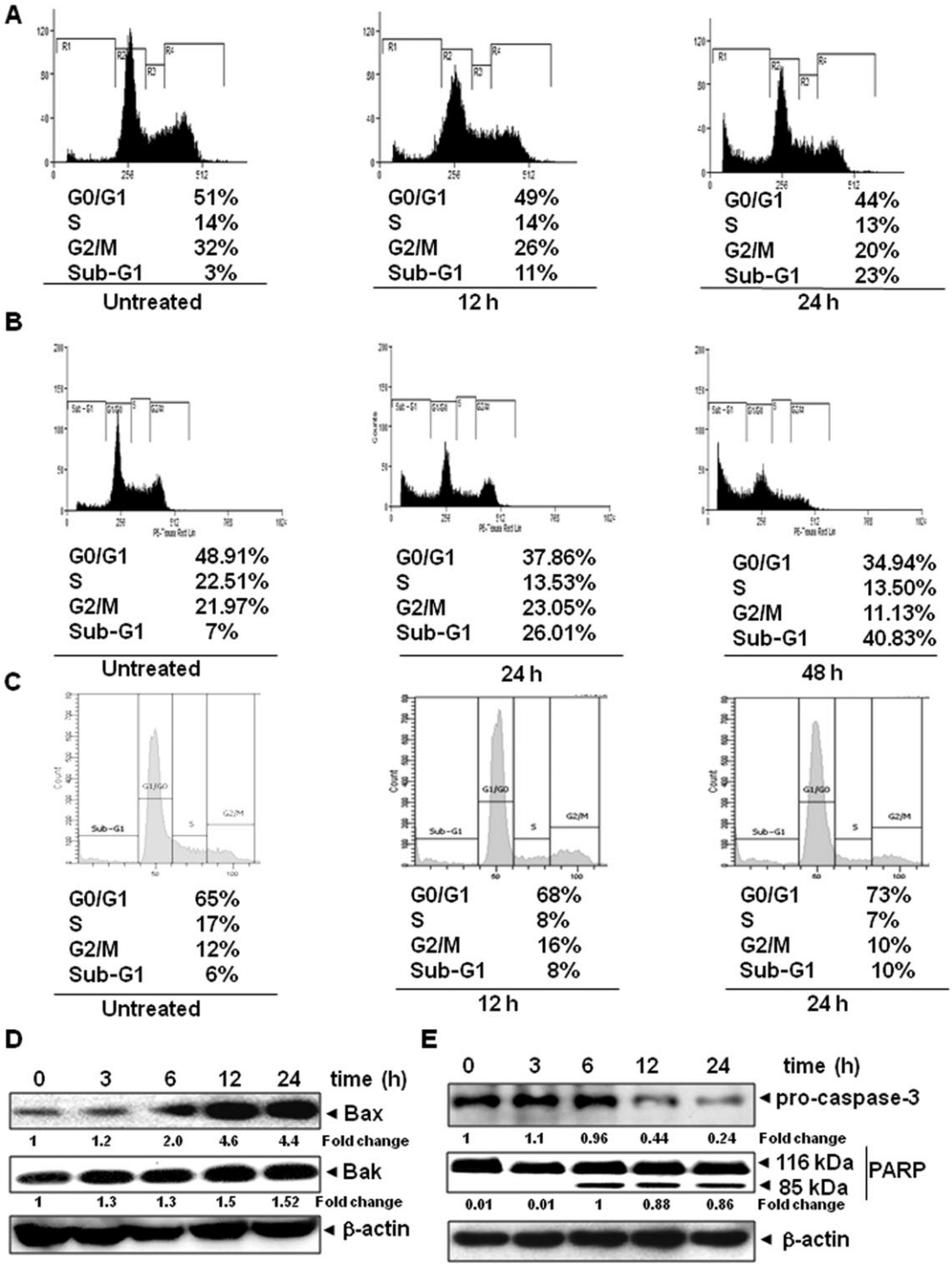

Figure 3

Celastrol causes accumulation of MM cells in the sub-G1 phase, increases the expression of pro-apoptotic proteins and activates caspase-3. (A) U266 cells (2×10^6 mL^{-1}) were treated with 1 μM celastrol for 0, 12 or 24 h, after which the cells were washed, fixed, stained with PI, and analysed for DNA content by flow cytometry. (B) RPMI 8266 cells resistant to bortezomib were treated with 1 μM celastrol for 0, 24 or 48 h, after which the cells were washed, fixed, stained with PI, and analysed for DNA content by flow cytometry. (C) Mouse embryonic fibroblast cells were treated with 1 μM celastrol for 0, 12 or 24 h, after which the cells were washed, fixed, stained with PI, and analysed for DNA content by flow cytometry. (D) U266 cells were treated with 1 μM celastrol for the indicated times, whole-cell extracts were prepared, separated on SDS-PAGE, and subjected to Western blot using antibodies against Bax and Bak. (E) U266 cells were treated as described in (C), whole-cell extracts were prepared, separated on SDS-PAGE, and subjected to Western blot using antibodies against indicated proteins. The same blots were stripped and reprobed with β-actin antibody to show equal protein loading. The cleaved bands in PARP were used for densitometric analysis.

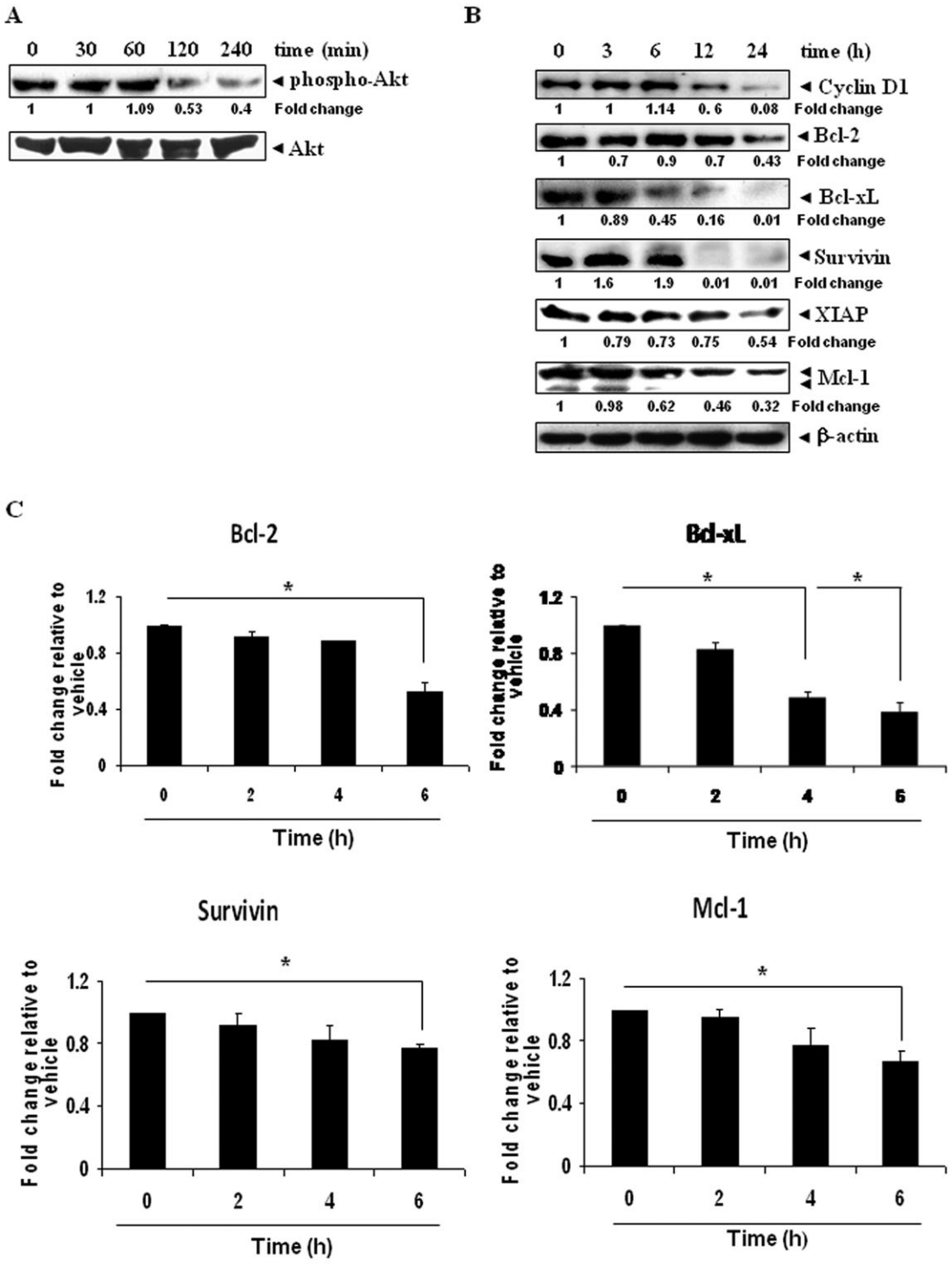

Figure 4

Celastrol suppresses Akt activation and inhibits the expression of anti-apoptotic proteins in MM cells. (A) U266 cells (2×10^6 mL^{-1}) were treated with 2.5 μM celastrol for the indicated times, whole-cell extracts were prepared, separated on SDS-PAGE, and subjected to Western blotting with phospho-Akt antibody. The same blots were stripped and reprobed with Akt antibody to show equal protein loading. (B) U266 cells were treated with 1 μM celastrol for the indicated times, whole-cell extracts were prepared, separated on SDS-PAGE, and subjected to antibodies against the indicated proteins. The same blots were stripped and reprobed with β-actin antibody to show equal protein loading. (C) U266 cells were treated with 1 μM celastrol for the indicated time intervals, after which RNA samples were extracted and used for real time PCR as described in Methods with 18S RNA as endogenous control. Results were analysed using Sequence Detection Software version 1.3 provided by Applied Biosystems. Relative gene expression was obtained after normalization with endogenous 18S RNA and determination of the difference in threshold cycle (Ct) between treated and untreated cells using 2-ΔΔCt method. The results shown are representative of three independent experiments.

support the predictive analysis seen with NF-κB inhibition on these markers (shown in Figure 1C, upper panel).

Celastrol inhibits constitutively active NF-κB in MM cells

The expression of various anti-apoptotic proteins is regulated by NF-κB (Sethi and Tergaonkar, 2009), therefore, the effect of celastrol on constitutive NF-κB activation in MM cells was examined. By using a DNA binding ELISA kit, we found that treatment of MM cells with celastrol suppressed constitutive active NF-κB in a time-dependent manner in both U266 (Figure 5A, left panel), and RPMI 8826 (Figure 5A, right panel) cells. Celastrol also suppressed the phosphorylation and degradation of IκBα (Figure 5B, left panel) and the phosphorylation and nuclear translocation of p65 in a time-dependent manner (Figure 5B, right panel).

The suppressive effect of celastrol on p65 nuclear translocation was also examined by immunocytochemistry. The results indicate that celastrol inhibited the appearance of p65 in the nucleus (Figure 5C). To determine whether the inhibition of NF-κB by celastrol resulted from inhibition of IKK, Western blot analysis was performed using phospho IKKα/β antibody. Celastrol inhibited IKK phosphorylation without affecting the levels of IKKα protein (Figure 5D).

Celastrol inhibits constitutively active and inducible STAT3 activation in MM cells

To determine whether celastrol can also modulate STAT3 activation, we exposed U266 cells to various doses of celastrol and for various times and assessed the levels of phosphorylated STAT3 by Western blotting. STAT3 was found to be constitutively active and celastrol down-regulated phospho-STAT3 levels in a dose- and time-dependent manner (Figure 6A). To confirm whether celastrol can suppress nuclear translocation of STAT3, we stained cells with anti-STAT3 antibody and found that exposure to celastrol substantially inhibited the translocation of STAT3 from the cytoplasm into the nucleus (Figure 6B).

STAT3 has been reported to be activated by soluble tyrosine kinases of the Src kinase families (Schreiner *et al.*, 2002). Hence, we determined whether celastrol can affect constitutive activation of Src kinase in U266 cells. We found that celastrol suppressed the constitutive phosphorylation of Src kinase in a time-dependent manner (Figure 6C, left panel). We also observed that JAK2 was constitutively active in U266 cells and pretreatment with celastrol suppressed this phosphorylation in a time-dependent manner, with maximum inhibition observed at 4 h (Figure 6C, right panel).

IL-6 is known to activate STAT3, therefore, we determined whether celastrol affects STAT3 activation induced by IL-6. IL-6 induced phospho-STAT3 in RPMI 8266 cells as early as 5 min (Figure 6D, left panel) after exposure and treatment with celastrol led to suppression of IL-6-induced phosphorylation of STAT3 in a time-dependent manner (Figure 6D, right panel). These results suggest that celastrol can down-regulate both constitutive and inducible STAT3 activation and corroborate with the predictive data on STAT3 inhibition as shown in Figure 1B, lower panel.

Discussion

The aim of this study was to determine whether celastrol could suppress the proliferation of MM cells by interfering with NF-κB and STAT3 pathways. Celastrol inhibited the proliferation of human MM cell lines regardless of whether they were sensitive or resistant to the conventional chemotherapeutic agents and synergistically enhanced the apoptotic effects of thalidomide and bortezomib. This triterpene also induced sub-G1 accumulation, leading to caspase-3 activation that correlated with the down-regulation of various proliferative and anti-apoptotic gene products. These effects of celastrol were found to be mediated through suppression of constitutively active NF-κB induced by inhibition of IKK phosphorylation. Celastrol also suppressed both constitutive and inducible STAT3 activation in MM cells concomitant with the inhibition of c-Src and JAK2 activation. This hypothesis was also tested in a virtual predictive tumour cell system and the predictive results indicate that celastrol mediates its suppressive effects on both NF-κB and STAT3 in MM cells primarily through inhibition of HSP90 and induction of HO-1 activities and this mechanism of action generated similar biomarker trends, as seen experimentally with celastrol effects on MM cells.

In agreement with previous reports (Feinman *et al.*, 1999; Bhardwaj *et al.*, 2007; Keats *et al.*, 2007), we found that MM cell lines expressed constitutively activated NF-κB, and that celastrol suppressed this activation. Although celastrol has been shown to inhibit NF-κB activation in various tumour cell lines (Sethi *et al.*, 2007a; Salminen *et al.*, 2010), how celastrol can inhibit constitutively activated NF-κB in MM cell lines has not been previously studied. Celastrol was found to inhibit NF-κB activation by suppressing the phosphorylation of IKK, which led to the inhibition of phosphorylation of both IκBα and p65. We also observed that celastrol suppressed constitutively active Akt. Both Akt and IKK have been shown to phosphorylate p65 (Sizemore *et al.*, 1999; Sethi *et al.*, 2008) and thus may contribute to inhibitory effect of celastrol on p65 phosphorylation.

In addition to NF-κB, we report for the first time that celastrol suppresses both constitutive and inducible STAT3 activation in MM cells, concomitant with inhibition of upstream Src and JAK2 kinases. STAT3 phosphorylation plays a critical role in the proliferation and survival of different tumour cells (Yue and Turkson, 2009). Previous studies have indicated that Src and JAK2 kinase activities co-operate to mediate constitutive activation of STAT3 (Campbell *et al.*, 1997; Garcia *et al.*, 2001). Our observations suggest that celastrol may block the co-operation of Src with JAKs involved in the tyrosyl phosphorylation of STAT3. We further observed that STAT3 activation induced by IL-6 treatment was also suppressed by celastrol. However, it is possible that celastrol gradually accumulates in the cells due to a relatively slow uptake process and hence inhibition of inducible STAT3 activation was observed only after 2 h pretreatment. Overall, it was found that this triterpene could suppress both constitutive and inducible STAT3 activation leading to other downstream effects as confirmed through the corroboration between the experimental and predictive data.

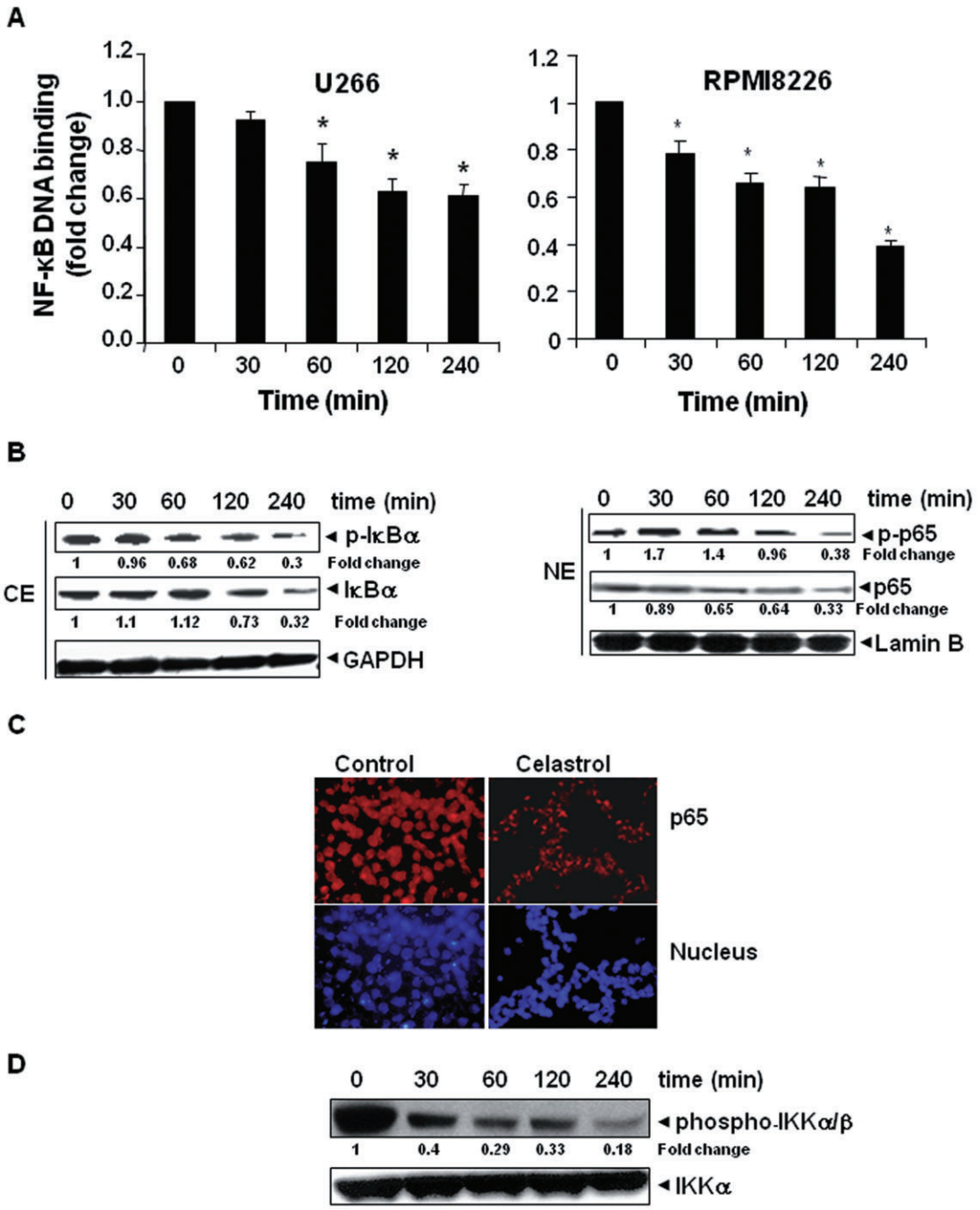

Figure 5

Celastrol inhibits constitutively active NF-κB in MM cells. Celastrol suppressed NF-κB in a time-dependent dependent manner in U266, and RPMI 8826 cells. (A, left panel) U266 cells (2×10^6 mL^{-1}) were treated with 2.5 μM celastrol for 0, 30, 60, 120 and 240 min; nuclear extracts were prepared, and 20 μg of the nuclear extract protein was used for ELISA-based DNA binding assay as described in Methods. (A, right panel) RPMI 8826 cells (2×10^6 mL^{-1}) were treated with 2.5 μM celastrol for 0, 30, 60, 120 and 240 min; DNA binding assay for NF-κB was performed. The results shown are representative of three independent experiments. (B, left panel) U266 cells were treated with 2.5 μM celastrol for 0, 30, 60, 120 and 240 min. Cytoplasmic extracts were prepared and Western blotting was done using phospho-IκBα and anti-IκBα antibodies. Equal protein loading and purity was evaluated by Western blotting against GAPDH. (B, right panel) U266 cells were treated with 2.5 μM celastrol for 0, 30, 60, 120 and 240 min. Nuclear extracts were prepared and Western blotting was done using antibodies for phospho-p65 and p65. Equal protein loading and purity was evaluated by Western blotting against lamin B. (C) U266 cells were incubated with medium or with 2.5 μM celastrol for 4 h and then analysed for the intracellular distribution of p65 by immunocytochemistry. Red indicates p65, and blue indicates nuclei (original magnification × 200). The results shown are representative of three independent experiments. (D) U266 cells were treated with 2.5 μM celastrol for 0, 30, 60, 120 and 240 min. Whole cell extracts were prepared and probed for phosphor-specific IKKα/β protein. Equal protein loading was evaluated by IKKα.

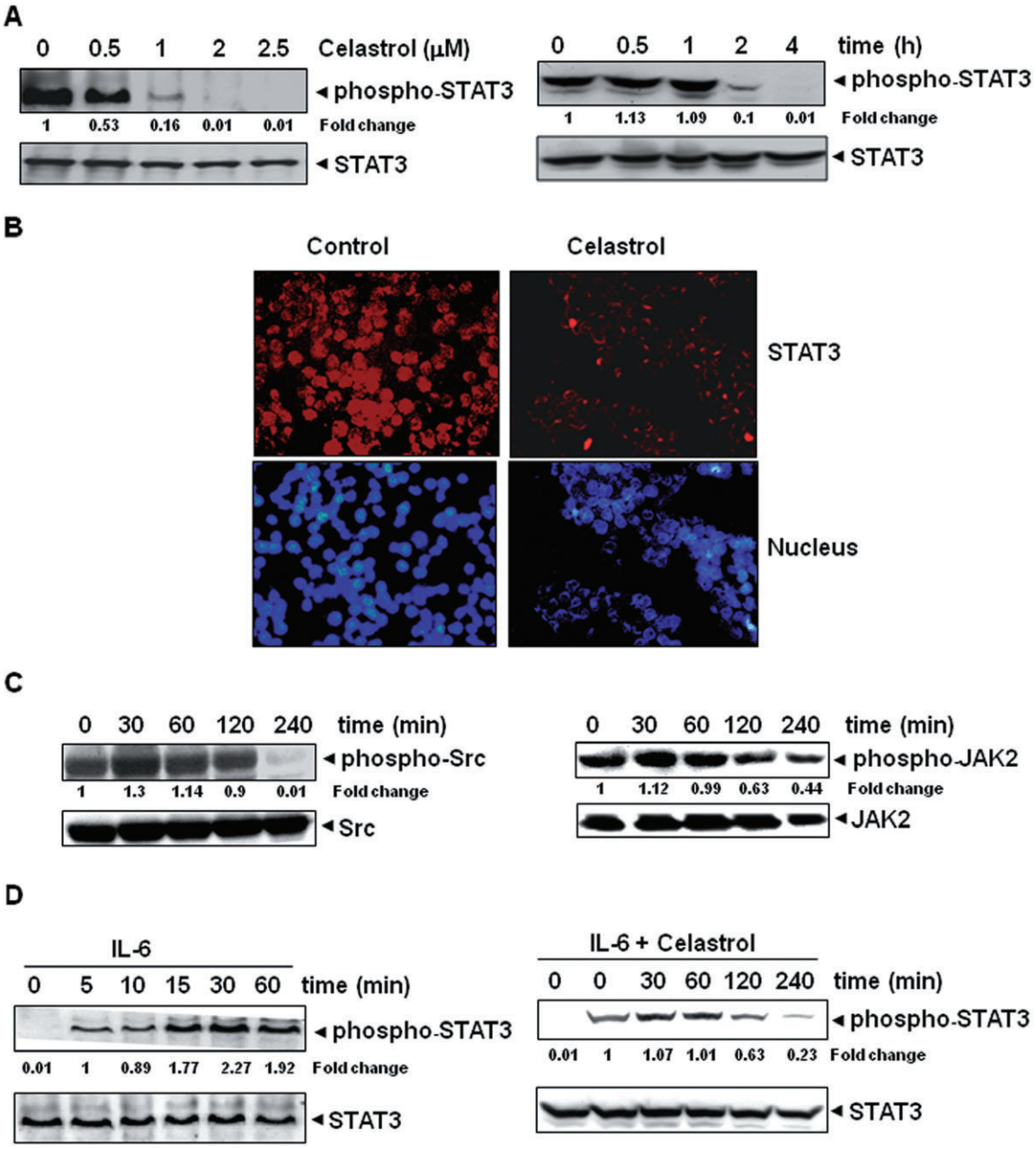

Figure 6

Celastrol inhibits constitutively active and IL-6 inducible STAT3 activation in MM cells. Celastrol suppressed phospho-STAT3 levels in a dose- and time-dependent manner. (A, left panel) U266 cells (2×10^6 mL^{-1}) were treated with indicated concentrations of celastrol for 4 h, after which whole-cell extracts were prepared, resolved on 7.5% SDS-PAGE gel, and probed with phospho-STAT3 antibody. The same blots were stripped and reprobed with STAT3 antibody to verify equal protein loading. (A, right panel) U266 cells (2×10^6 mL^{-1}) were treated with the 2.5 μM celastrol for indicated time points, after which Western blotting was performed. (B) U266 cells (1×10^5 mL^{-1}) were incubated with 2.5 μM celastrol for 4 h and then analysed for the intracelullar distribution of STAT3 by immunocytochemistry. Red indicates STAT3, and blue indicates nucleus (original magnification × 200). (C) U266 cells (2×10^6 mL^{-1}) were treated with 2.5 μM celastrol for indicated time intervals, after which whole-cell extracts were prepared, resolved on 10% SDS-PAGE, and probed with phospho-Src and phospho-JAK-2 antibodies. The same blots were stripped and reprobed with Src and JAK2 antibodies to verify equal protein loading. (D, left panel) RPMI 8226 cells (2×10^6 mL^{-1}) were treated with IL-6 (10 ng·mL^{-1}) for indicated times, whole cell extracts were prepared, and phospho-STAT3 was detected by Western blot analysis. The same blots were stripped and reprobed with STAT3 antibody to verify equal protein loading. (D, right panel) RPMI 8226 cells were treated with 2.5 μM celastrol for the indicated times and then stimulated with IL-6 (10 ng·mL^{-1}) for 15 min. Whole-cell extracts were then prepared and analysed for phospho-STAT3 by Western blotting. The same blots were stripped and reprobed with STAT3 antibody to verify equal protein loading.

Whether suppression of STAT3 activation by celastrol is linked to inhibition of NF-κB activation is not clear. A recent study indicated that STAT3 prolongs the nuclear retention of NF-κB through acetyltransferase p300-mediated RelA acetylation, thereby interfering with NF-κB nuclear export (Lee *et al.*, 2009). STAT3 and NF-κB, however, are activated in response to different cytokines: IL-6 is a major inducer of STAT3 phosphorylation whereas TNF is a potent activator of NF-κB. Moreover erythropoietin, a glycoprotein hormone has been shown to activate NF-κB through the activation of JAK2 kinase (Digicaylioglu and Lipton, 2001). Thus, it is possible that the suppression of JAK2 kinase activation is the critical target for the inhibition of both NF-κB and STAT3 activation by celastrol. Based on our predictive analysis, inhibition of NF-κB and STAT3 can be attributed to the downstream effects of HSP90 inhibition and HO-1 induction by celastrol in MM cells.

We also found that celastrol suppressed several genes that are regulated by NF-κB and STAT3; including the proliferative (cyclin D1) and anti-apoptotic gene products (Bcl-2, Bcl-xL, survivin, XIAP and Mcl-1) in MM cells. Constitutively active STAT3 has been implicated in the induction of resistance to apoptosis (Aggarwal *et al.*, 2009), possibly through the expression of Bcl-2 and cyclin D1 (Aggarwal *et al.*, 2006). Bcl-xL can block cell death induced by variety of chemotherapeutic agents (Li and Sethi, 2010), and expression of Bcl-xL has been correlated with chemoresistance in patients with MM (Tu *et al.*, 1998). The down-regulation of Bcl-2, Bcl-xL, survivin, XIAP and Mcl-1 expression is probably linked to the ability of celastrol to induce apoptosis in MM cells. To our knowledge, this is the first report of the ability of celastrol to overcome chemotherapy-induced resistance in MM cells. Celastrol-induced cell death in the RPMI 8226 cell line resistant to bortezomib was comparable to its drug-sensitive counterpart. Celastrol has been recently reported to enhance TNF-related apoptosis-inducing ligand-induced cell death in various tumour cells by down-regulation of various cell survival proteins (Sung *et al.*, 2010; Zhu *et al.*, 2010) and also induce apoptosis in imatinib-resistant chronic myeloid leukaemia cells harbouring the T315I mutation (Lu *et al.*, 2010). Thus, it is possible that celastrol sensitizes MM cells to bortezomib and other chemotherapeutic drugs by down-regulating the effects of NF-κB and STAT3 on various cell survival proteins.

Both bortezomib and thalidomide, used for the treatment of MM patients, can suppress NF-κB activation but also exert severe side effects (Hideshima *et al.*, 2000; Richardson *et al.*, 2006). In preclinical studies using various inflammatory diseases and cancer models, celastrol has been shown to be well-tolerated with no reported toxicity so far (Sethi *et al.*, 2007a; Huang *et al.*, 2008; Dai *et al.*, 2009; Lu *et al.*, 2010; Pang *et al.*, 2010; Paris *et al.*, 2010). Thus, in conclusion, safety information from preclinical studies and the ability of celastrol to suppress NF-κB and STAT3 activation, down-regulate the expression of various cell survival proteins, to synergistically potentiate the effects of thalidomide and bortezomib, and to overcome drug resistance provides a sound basis for conducting clinical trials with celastrol, alone or in combination with other agents, to enhance treatment efficacy and to overcome chemoresistance in MM patients.

Acknowledgements

This work was supported by grants from National Medical Research Council of Singapore [Grant R-184-000-201-275] and from Academic Research Fund [Grant R-184-000-177-112] to G. S. C. W. J. was supported by grants from National Medical Research Council Clinician Scientist Awards as well as grants from the National Medical Research Council [Grants EDG-0025-008; EDG-0055-2009; EDG-0068-2009], Ministry of Education [MOE-2009-T2-2-073], the National University Cancer Institute Center Grant, and the Cancer Science Institute of Singapore, Experimental Therapeutics II Program [Grant R-713-002-011-271]. A. P. K. was supported by grants from the National Medical Research Council of Singapore [Grant R-713-000-124-213] and Cancer Science Institute of Singapore, Experimental Therapeutics I Program [Grant R-713-001-011-271].

Conflict of interest

None declared.

References

Aggarwal BB, Sethi G, Ahn KS, Sandur SK, Pandey MK, Kunnumakkara AB *et al.* (2006). Targeting signal-transducer-and-activator-of-transcription-3 for prevention and therapy of cancer: modern target but ancient solution. Ann N Y Acad Sci 1091: 151–169.

Aggarwal BB, Vijayalekshmi RV, Sung B (2009). Targeting inflammatory pathways for prevention and therapy of cancer: short-term friend, long-term foe. Clin Cancer Res 15: 425–430.

Bhardwaj A, Sethi G, Vadhan-Raj S, Bueso-Ramos C, Takada Y, Gaur U *et al.* (2007). Resveratrol inhibits proliferation, induces apoptosis, and overcomes chemoresistance through down-regulation of STAT3 and nuclear factor-κB-regulated antiapoptotic and cell survival gene products in human multiple myeloma cells. Blood 109: 2293–2302.

Bharti AC, Donato N, Singh S, Aggarwal BB (2003). Curcumin (diferuloylmethane) down-regulates the constitutive activation of nuclear factor-kappa B and IkappaBalpha kinase in human multiple myeloma cells, leading to suppression of proliferation and induction of apoptosis. Blood 101: 1053–1062.

Campbell GS, Yu CL, Jove R, Carter-Su C (1997). Constitutive activation of JAK1 in Src-transformed cells. J Biol Chem 272: 2591–2594.

Catlett-Falcone R, Landowski TH, Oshiro MM, Turkson J, Levitzki A, Savino R *et al.* (1999). Constitutive activation of Stat3 signaling confers resistance to apoptosis in human U266 myeloma cells. Immunity 10: 105–115.

Cavo M, Baccarani M (2006). The changing landscape of myeloma therapy. N Engl J Med 354: 1076–1078.

Cirstea D, Hideshima T, Rodig S, Santo L, Pozzi S, Vallet S *et al.* (2010). Dual inhibition of akt/mammalian target of rapamycin pathway by nanoparticle albumin-bound-rapamycin and perifosine induces antitumor activity in multiple myeloma. Mol Cancer Ther 9: 963–975.

Conticello C, Giuffrida R, Adamo L, Anastasi G, Martinetti D, Salomone E *et al*. (2011). NF-kappaB localization in multiple myeloma plasma cells and mesenchymal cells. Leuk Res 35: 52–60.

Dai Y, DeSano JT, Meng Y, Ji Q, Ljungman M, Lawrence TS *et al*. (2009). Celastrol potentiates radiotherapy by impairment of DNA damage processing in human prostate cancer. Int J Radiat Oncol Biol Physics 74: 1217–1225.

Digicaylioglu M, Lipton SA (2001). Erythropoietin-mediated neuroprotection involves cross-talk between Jak2 and NF-kappaB signalling cascades. Nature 412: 641–647.

Feinman R, Koury J, Thames M, Barlogie B, Epstein J, Siegel DS (1999). Role of NF-κB in the rescue of multiple myeloma cells from glucocorticoid-induced apoptosis by bcl-2. Blood 93: 3044–3052.

Garcia R, Bowman TL, Niu G, Yu H, Minton S, Muro-Cacho CA *et al*. (2001). Constitutive activation of Stat3 by the Src and JAK tyrosine kinases participates in growth regulation of human breast carcinoma cells. Oncogene 20: 2499–2513.

Glasmacher A, Hahn C, Hoffmann F, Naumann R, Goldschmidt H, von Lilienfeld-Toal M *et al*. (2006). A systematic review of phase-II trials of thalidomide monotherapy in patients with relapsed or refractory multiple myeloma. Br J Haematol 132: 584–593.

Hideshima T, Chauhan D, Shima Y, Raje N, Davies FE, Tai YT *et al*. (2000). Thalidomide and its analogs overcome drug resistance of human multiple myeloma cells to conventional therapy. Blood 96: 2943–2950.

Huang Y, Zhou Y, Fan Y, Zhou D (2008). Celastrol inhibits the growth of human glioma xenografts in nude mice through suppressing VEGFR expression. Cancer Lett 264: 101–106.

Jagannath S (2005). Novel agents in first-line therapy for myeloma: from the multiple myeloma research foundation. Oncology 19: 1551–1554.

Jagannath S, Kyle R, Palumbo A, Siegel D, Cunningham S, Berenson J (2010). The current status and future of multiple myeloma in the clinic. Clin Lymphoma Myeloma 10: E1–E16.

Kannaiyan R, Shanmugam MK, Sethi G (2010). Molecular targets of celastrol derived from Thunder of God Vine: potential role in the treatment of inflammatory disorders and cancer. Cancer Lett 303: 9–20.

Kawano M, Hirano T, Matsuda T, Taga T, Horii Y, Iwato K *et al*. (1988). Autocrine generation and requirement of BSF-2/IL-6 for human multiple myelomas. Nature 332: 83–85.

Keats JJ, Fonseca R, Chesi M, Schop R, Baker A, Chng WJ *et al*. (2007). Promiscuous mutations activate the noncanonical NF-kappaB pathway in multiple myeloma. Cancer Cell 12: 131–144.

Kumar AP, Quake AL, Chang MK, Zhou T, Lim KS, Singh R *et al*. (2009). Repression of NHE1 expression by PPARgamma activation is a potential new approach for specific inhibition of the growth of tumor cells in vitro and in vivo. Cancer Res 69: 8636–8644.

Kumar S, Rajkumar SV (2006). Thalidomide and lenalidomide in the treatment of multiple myeloma. Eur J Cancer 42: 1612–1622.

Kyle RA, Rajkumar SV (2004). Drug therapy: multiple myeloma. N Engl J Med 351: 1860–1873 + 1921.

Kyle RA, Rajkumar SV (2008). Multiple myeloma. Blood 111: 2962–2972.

Lee H, Herrmann A, Deng JH, Kujawski M, Niu G, Li Z *et al*. (2009). Persistently activated Stat3 maintains constitutive NF-kappaB activity in tumors. Cancer Cell 15: 283–293.

Li F, Sethi G (2010). Targeting transcription factor NF-κB to overcome chemoresistance and radioresistance in cancer therapy. Biochim Biophys Acta – Rev Cancer 1805: 167–180.

Li F, Fernandez PP, Rajendran P, Hui KM, Sethi G (2010). Diosgenin, a steroidal saponin, inhibits STAT3 signaling pathway leading to suppression of proliferation and chemosensitization of human hepatocellular carcinoma cells. Cancer Lett 292: 197–207.

Li-Weber M (2010). Targeting apoptosis pathways in cancer by Chinese medicine. Cancer Lett [Epub ahead of print].

Lu Z, Jin Y, Qiu L, Lai Y, Pan J (2010). Celastrol, a novel HSP90 inhibitor, depletes Bcr-Abl and induces apoptosis in imatinib-resistant chronic myelogenous leukemia cells harboring T315I mutation. Cancer Lett 290: 182–191.

Morita H, Hirasawa Y, Muto A, Yoshida T, Sekita S, Shirota O (2008). Antimitotic quinoid triterpenes from Maytenus chuchuhuasca. Bioorg Med Chem Lett 18: 1050–1052.

Ni H, Ergin M, Huang Q, Qin JZ, Amin HM, Martinez RL *et al*. (2001). Analysis of expression of nuclear factor κB (NF-κB) in multiple myeloma: downregulation of NF-κB induces apoptosis. Br J Haematol 115: 279–286.

Pang X, Yi Z, Zhang J, Lu B, Sung B, Qu W *et al*. (2010). Celastrol suppresses angiogenesis-mediated tumor growth through inhibition of AKT/mammalian target of rapamycin pathway. Cancer Res 70: 1951–1959.

Paris D, Ganey NJ, Laporte V, Patel NS, Beaulieu-Abdelahad D, Bachmeier C *et al*. (2010). Reduction of β-amyloid pathology by celastrol in a transgenic mouse model of Alzheimer's disease. J Neuroinflammation 7: 1–15.

Raab MS, Podar K, Breitkreutz I, Richardson PG, Anderson KC (2009). Multiple myeloma. Lancet 374: 324–339.

Renard P, Ernest I, Houbion A, Art M, Le Calvez H, Raes M *et al*. (2001). Development of a sensitive multi-well colorimetric assay for active NFkappaB. Nucleic Acids Res 29: E21.

Richardson PG, Briemberg H, Jagannath S, Wen PY, Barlogie B, Berenson J *et al*. (2006). Frequency, characteristics, and reversibility of peripheral neuropathy during treatment of advanced multiple myeloma with bortezomib. J Clin Oncol 24: 3113–3120.

Roy KR, Reddy GV, Maitreyi L, Agarwal S, Achari C, Vali S *et al*. (2010). Celecoxib inhibits MDR1 expression through COX-2-dependent mechanism in human hepatocellular carcinoma (HepG2) cell line. Cancer Chemother Pharmacol 65: 903–911.

Salminen A, Lehtonen M, Paimela T, Kaarniranta K (2010). Celastrol: molecular targets of Thunder God Vine. Biochem Biophys Res Commun 394: 439–442.

Schreiner SJ, Schiavone AP, Smithgall TE (2002). Activation of STAT3 by the Src family kinase Hck requires a functional SH3 domain. J Biol Chem 277: 45680–45687.

Sethi G, Tergaonkar V (2009). Potential pharmacological control of the NF-κB pathway. Trends Pharmacol Sci 30: 313–321.

Sethi G, Ahn KS, Pandey MK, Aggarwal BB (2007a). Celastrol, a novel triterpene, potentiates TNF-induced apoptosis and suppresses invasion of tumor cells by inhibiting NF-kappaB-regulated gene products and TAK1-mediated NF-kappaB activation. Blood 109: 2727–2735.

Sethi G, Kwang SA, Pandey MK, Aggarwal BB (2007b). Celastrol, a novel triterpene, potentiates TNF-induced apoptosis and suppresses invasion of tumor cells by inhibiting NF-κB-regulated gene products and TAK1-mediated NF-κB activation. Blood 109: 2727–2735.

Sethi G, Ahn KS, Sung B, Kunnumakkara AB, Chaturvedi MM, Aggarwal BB (2008). SH-5, an AKT inhibitor potentiates apoptosis and inhibits invasion through the suppression of anti-apoptotic, proliferative and metastatic gene products regulated by IkappaBalpha kinase activation. Biochem Pharmacol 76: 1404–1416.

Shah JJ, Orlowski RZ (2009). Proteasome inhibitors in the treatment of multiple myeloma. Leukemia 23: 1964–1979.

Sizemore N, Leung S, Stark GR (1999). Activation of phosphatidylinositol 3-kinase in response to interleukin-1 leads to phosphorylation and activation of the NF-kappaB p65/RelA subunit. Mol Cell Biol 19: 4798–4805.

Sung B, Kunnumakkara AB, Sethi G, Anand P, Guha S, Aggarwal BB (2009). Curcumin circumvents chemoresistance in vitro and potentiates the effect of thalidomide and bortezomib against human multiple myeloma in nude mice model. Mol Cancer Ther 8: 959–970.

Sung B, Park B, Yadav VR, Aggarwal BB (2010). Celastrol, a triterpene, enhances TRAIL-induced apoptosis through the down-regulation of cell survival proteins and up-regulation of death receptors. J Biol Chem 285: 11498–11507.

Tan SM, Li F, Rajendran P, Kumar AP, Hui KM, Sethi G (2010). Identification of beta-escin as a novel inhibitor of signal transducer and activator of transcription 3/Janus-activated kinase 2 signaling pathway that suppresses proliferation and induces apoptosis in human hepatocellular carcinoma cells. J Pharmacol Exp Ther 334: 285–293.

Tu Y, Renner S, Xu FH, Fleishman A, Taylor J, Weisz J *et al.* (1998). BCL-X expression in multiple myeloma: possible indicator of chemoresistance. Cancer Res 58: 256–262.

Vali S, Pallavi R, Kapoor S, Tatu U (2010). Virtual prototyping study shows increased ATPase activity of Hsp90 to be the key determinant of cancer phenotype. Syst Synth Biol 4: 25–33.

Yadav VR, Sung B, Prasad S, Kannappan R, Cho SG, Liu M *et al.* (2010). Celastrol suppresses invasion of colon and pancreatic cancer cells through the downregulation of expression of CXCR4 chemokine receptor. J Mol Med 88: 1243–1253.

Yamaguchi H, Wang HG (2001). The protein kinase PKB/Akt regulates cell survival and apoptosis by inhibiting Bax conformational change. Oncogene 20: 7779–7786.

Yu X, Tao W, Jiang F, Li C, Lin J, Liu C (2010). Celastrol attenuates hypertension-induced inflammation and oxidative stress in vascular smooth muscle cells via induction of heme oxygenase-1. Am J Hypertens 23: 895–903.

Yue P, Turkson J (2009). Targeting STAT3 in cancer: how successful are we? Expert Opin Investig Drugs 18: 45–56.

Zhang D, Xu L, Cao F, Wei T, Yang C, Uzan G *et al.* (2010). Celastrol regulates multiple nuclear transcription factors belonging to HSP90's clients in a dose- and cell type-dependent way. Cell Stress Chaperones 15: 939–946.

Zhu H, Ding WJ, Wu R, Weng QJ, Lou JS, Jin RJ *et al.* (2010). Synergistic anti-cancer activity by the combination of TRAIL/APO-2L and celastrol. Cancer Invest 28: 23–32.